Dual-pH Sensitive Charge-Reversal Polypeptide Micelles for Tumor-Triggered Targeting Uptake and Nuclear Drug Delivery

*Shi-Song Han, Ze-Yong Li, Jing-Yi Zhu, Kai Han, Zheng-Yang Zeng, Wei Hong, Wen-Xin Li, Hui-Zhen Jia, Yun Liu, Ren-Xi Zhuo, and Xian-Zheng Zhang**

***A** novel dual-pH sensitive charge-reversal strategy is designed to deliver antitumor drugs targeting to tumor cells and to further promote the nuclei internalization by a stepwise response to the mildly acidic extracellular pH (≈6.5) of a tumor and endo/lysosome pH (≈5.0). Poly(L-lysine)-block–poly(L-leucine) diblock copolymer is synthesized and the lysine amino residues are amidated by 2,3-dimethylmaleic anhydride to form β-carboxylic amide, making the polypeptides self-assemble into negatively charged micelles. The amide can be hydrolyzed when exposed to the mildly acidic tumor extracellular environment, which makes the micelles switch to positively charged and they are then readily internalized by tumor cells. A nuclear targeting Tat peptide is further conjugated to the polypeptide via a click reaction. The Tat is amidated by succinyl chloride to mask its positive charge and cell-penetrating function and thus to inhibit nonspecific cellular uptake. After the nanoparticles are internalized into the more acidic intracellular endo/lysosomes, the Tat succinyl amide is hydrolyzed to reactivate the Tat nuclear targeting function, promoting nanoparticle delivery into cell nuclei. This polypeptide nanocarrier facilitates tumor targeting and nuclear delivery simultaneously by simply modifying the lysine amino residues of polylysine and Tat into two different pH-sensitive β-carboxylic amides.*

1. Introduction

Chemotherapy acts a significant role in tumor therapy and has received great attention in the past decades. But traditional antitumor drug systems still suffer from severe obstacles such as indistinguishable from healthy and tumor tissues and nonspecific drug internalization all over the body, which cause disappointing low therapeutic efficacy and fatal side effects.[1,2] Targeting delivery of drugs emerges as a significant method to specifically transport the antitumor drugs to tumors and decrease the normal tissues internalization, thus reducing the side effects and improving the clinical efficiency. Nowadays various targeting delivery systems have been developed and some have been already in clinical trials.[3] It is found that nanoparticles less than certain size (≈200 nm) can passively accumulate in tumor tissues after intravenous administration due to the enhanced permeability and retention effect.[4] The targeting efficiency can be further enhanced by actively conjugating targeting ligands such as antibody, peptide, folate, and biotin to drug delivery systems, which can be selectively recognized by overexpressed receptors on tumor cells.[5] However, normal tissues usually

S.-S. Han, Z.-Y. Li, J.-Y. Zhu, K. Han, H.-Z. Jia, Y. Liu, Prof. R.-X. Zhuo, Prof. X.-Z. Zhang
Key Laboratory of Biomedical Polymers of Ministry of Education and Department of Chemistry
Wuhan University
Wuhan 430072, P.R. China
E-mail: xz-zhang@whu.edu.cn

Z.-Y. Zeng, W. Hong, Prof. W.-X. Li
State Key Laboratory of Virology and College of Life Sciences
Wuhan University
Wuhan 430072, P.R. China

DOI: 10.1002/smll.201402865

also express the same receptors that recognize the targeting ligands just at a lower level,[6] which definitely compromise the targeting efficiency and therapeutic effects.

Stimuli-responsive delivery systems, which can undergo chemical or physical transformations once exposed to tumor microenvironments or external stimuli, have emerged as a smart and powerful strategy for targeting delivery and controlled release. Among the various stimuli such as pH, temperature, redox potential, enzymes, light, magnetic field and specific bioactive molecules,[2,8] pH responsivity is one of the most extensively exploited since pH values vary in different tissues and cellular compartments. It is found that tumor extracellular environment is more acidic (pH 6.2–6.9) than blood and normal tissues (pH 7.3–7.4),[9] while the pH value in cellular endo/lysosomes is even lower (4.0–6.0).[10] Recently, pH dependent charge reversal delivery systems, which can reverse their negative charge to positive charge upon pH stimuli, have been developed and exhibit great superiority in controlled release and targeted delivery of drugs. Noted that the surface charge of nanoparticles is proved to play a momentous role in the cell internalization and the blood stability.[11] The charge reversal nanocarriers can maintain their original negative charged status under neutral conditions in bloodstream thus inhibiting nonspecific interactions with serum proteins and normal tissues, but quickly convert into positively charged status once arriving at the tumor tissues or endo/lysosomes thus enhancing the tumor cell internalization and achieving the controlled release. Kataoka group have developed the endo/lysosome pH triggered charge reversal delivery systems for cytoplasm drug release,[12,13] while Shen group[14,15] and Wang group[16–18] further developed the tumor mildly acidic microenvironment triggered tumor targeting drug delivery, which exhibited obvious advantages and great potential in tumor targeting drug delivery.

Most antitumor drugs such as doxorubicin (DOX), camptothecin, and cisplatin exert their function by reacting with the DNA or inhibiting DNA topoisomerase to induce cell death.[19,20] These processes mainly occur in the cell nuclei, where the drugs have to reach to exert their therapeutic effect. Multidrug resistance (MDR) is nowadays one of the most challenging and complicated barriers in chemotherapy, since the therapeutic drugs are constantly pumped out from cytoplasm by the usually overexpressed P-glycoproteins which lead to extensively reduced therapeutic efficacy.[21,22] Therefore, delivery of antitumor drugs directly into cell nuclei will be of great significance to bypass the MDR effect and induce cell apoptosis more directly and efficiently.[23]

Tat peptide, derived from the protein transduction domain of human immunodeficiency virus (HIV) transactivator of transcription protein,[24] has been proved to have the capacity of actively transporting cargos into cell nuclei and thus has been exploited in many nuclear targeting delivery systems.[25,26] However, the cationic Tat peptide is also characterized by its cell penetrating capacity that quickly internalized by all cells, which inhibits its application in targeting delivery and in vivo studies.[27] Recently, a pH sensitive molecular modification strategy for Tat peptide was proposed to settle this problem.[28] The cell penetrating function of Tat peptide was shielded via amidating by succinyl chloride. When the nanoparticles were internalized and arrived at the acidic endo/lysosomes (pH ≈ 5.0), the β-carboxylic amide was hydrolyzed and the nuclear localization function of Tat recovered and then the nanocarriers delivered their cargos into cell nuclei. This strategy inhibits the nonspecific internalization of Tat peptide in bloodstream while preserves its nuclear targeting capacity once internalized in tumor cells.

In this study, a dual-pH sensitive charge reversal nanocarrier was designed for tumor triggered targeting internalization and nuclear delivery of antitumor drugs as shown in **Scheme 1**. Polypeptides which possess excellent biocompatibility and biodegradability were utilized here to form basic micelles to package hydrophobic drugs.[29] Amphiphilic diblock copolymer poly(L-lysine)-block–poly(L-leucine) (PLL–PLLeu) was synthesized by ring opening polymerization (ROP) of *N*-carboxyanhydrides (NCA) to assemble into positively charged micelles. Then the Tat peptide amidated by succinyl chloride (Tat(SA)) was conjugated via click reaction to provide the polypeptide the ability of endo/lysosome pH sensitive nuclear targeting function. Afterward, the lysine amino residues of the polylysine were amidated by 2,3-dimethylmaleic anhydride (DMA) into another β-carboxylic amide to form negative charged PLLeu–PLL(DMA)–Tat(SA) (PPDTS) micelles. The amides would be hydrolyzed once the nanoparticles reach the mildly acidic tumor extracellular environment (pH ≈ 6.5) and the micelles would switch to positive charged again and be quickly internalized by tumor cells. By simply modifying the lysine amino residues of polylysine and Tat with two different amidating reagents, respectively, this nanocarrier will facilitate the tumor targeting and nuclear delivery simultaneously.

2. Results and Discussion

2.1. Synthesis and Characterization of PPDTS

The detailed synthesis protocol of PPDTS was shown in **Scheme 2**. At first ε-benzyloxycarbonyl-L-lysine *N*-carboxyanhydride (LLZ–NCA) and L-leucine *N*-carboxyanhydride (LLeu–NCA) were prepared by Fuchs-Farthing method through reacting ε-benzyloxycarbonyl-L-lysine (LLZ) and L-leucine (LLeu) with recrystallized triphosgene (Scheme 2A).[30,31] The amphiphilic diblock polypeptide PLL–PLLeu was then synthesized by two-step ROP of the NCA and subsequent deprotection, while propargyl amine was used as the initiator to provide the polypeptide a terminal alkynyl group for further click reaction (Scheme 2B). The NMR spectra of LLeu–NCA, LLZ–NCA, poly(ε-benzyloxycarbonyl-L-lysine) (PLLZ), PLLZ–PLLeu, and PLL–PLLeu were shown in Figure S1, Supporting Information. Dimethyl sulphoxide (DMSO) -d_6 was used as solvent, and all characteristic peaks were assigned to the protons, which were in agreement with literature reports,[29,32] indicating the successful synthesis of every step. The feed ratios of LLZ–NCA to propargyl amine in polymerization were varied from 80:1, 54:1 to 36:1, and that of LLeu–NCA to LLZ–NCA were varied from 1:2.2, 1:3 to 1:6, and finally the polypeptide with the feed ratio of 1:54:25 was selected for the following experiments in consideration of

DOI: 10.1002/smll.201402865

small NANO MICRO

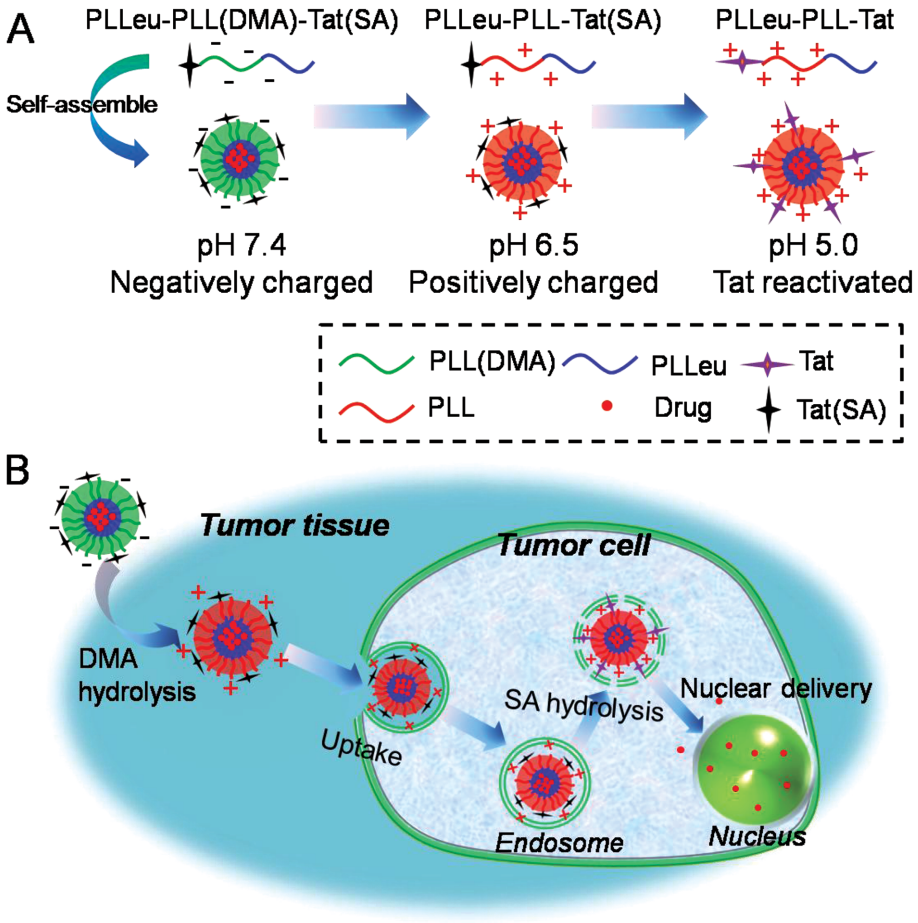

Scheme 1. Schematic illustration of A) the self-assembled polypeptide micelles stepwise responding to mildly acidic tumor tissues (pH ≈ 6.5) by undergoing a charge conversion process and more acidic endosomes (pH ≈ 5.0) that the nuclear location function of Tat peptide was reactivated; B) the tumor triggered cellular uptake of nanoparticles and nuclear delivery of drugs.

their solubility, assembly manner and cytotoxicity (data not shown). From the integration ratios of the characteristic resonance signals, the degree of polymerization (DP) ratio of leucine to lysine was calculated to be 1:2.3. The weight-average mole mass of PLLZ–PLL determined by gel permeation chromatography (GPC) in *N*,*N*′-dimethylformamide (DMF) was 17 370, so the DP of lysine and leucine were calculated to be 55 and 24, respectively.

The azido-terminated N_3–Tat peptide was synthesized manually by standard Fmoc solid phase peptide synthesis (SPPS) method as demonstrated in Scheme S1, Supporting Information and characterized by matrix-assisted laser desorption/ionization time of flight (MALDI–TOF) as shown in Figure S2A, Supporting Information.[33] The molecular mass of N_3–Tat was calculated to be 1641.9 and that measured was around 1640.9, indicating the successful synthesis. The weaker peak around *m*/*z* 1614 corresponded to a fraction of byproduct that some azide groups were reduced to amino group during peptide cleavage from the resin,[34] which could not be thoroughly avoided in the presence of thioscavenger, but it did not matter because the byproduct could not participate in the following click reaction and would be cleared out in the dialysis step. The Tat peptide was further reacted with succinyl chloride to amidate the lysine amino residues into acid-labile *β*-carboxylic amides (Scheme S1, Supporting Information) which would be hydrolyzed at pH 5.0 environments.[28] The N_3–Tat(SA) was also analyzed by MALDI–TOF. As shown in Figure S2B, Supporting Information, an increase of 200 or 300 of the molecular mass occurred compared to Tat peptide, implying that two lysine residues and a part of the glutamine residues were reacted. The two or three amino acids modification was reported sufficient to shield the positive charge of Tat and inhibit the nonspecific interaction with normal cells.[28]

Afterward the N_3–Tat(SA) was conjugated to the amphiphilic diblock polypeptide PLL–PLLeu via copper (I) catalyzed azide–alkyne cycloaddition (CuAAC) click reaction (Scheme 2C).[35] The Fourier transform-infrared spectroscopy (FTIR) spectra of PLL–PLLeu, N_3–Tat(SA), and PLLeu–PLL–Tat(SA) (PPTS) were shown in **Figure 1**A. The peak at around 2100 cm^{-1} that derived from alkynyl groups or azide groups disappeared in PPTS, indicating the successful reaction. The click reaction was further confirmed by the UV–vis spectra (Figure 1B) that the adsorption at 275 nm from tyrosine phenol group of Tat emerged for PPTS, while PLL–PLLeu did not.

Finally the PPDTS was obtained by reacting PPTS with DMA in basic aqueous solution (Scheme 2D).[17] The lysine amino groups of polylysine were modified to another

DOI: 10.1002/smll.201402865

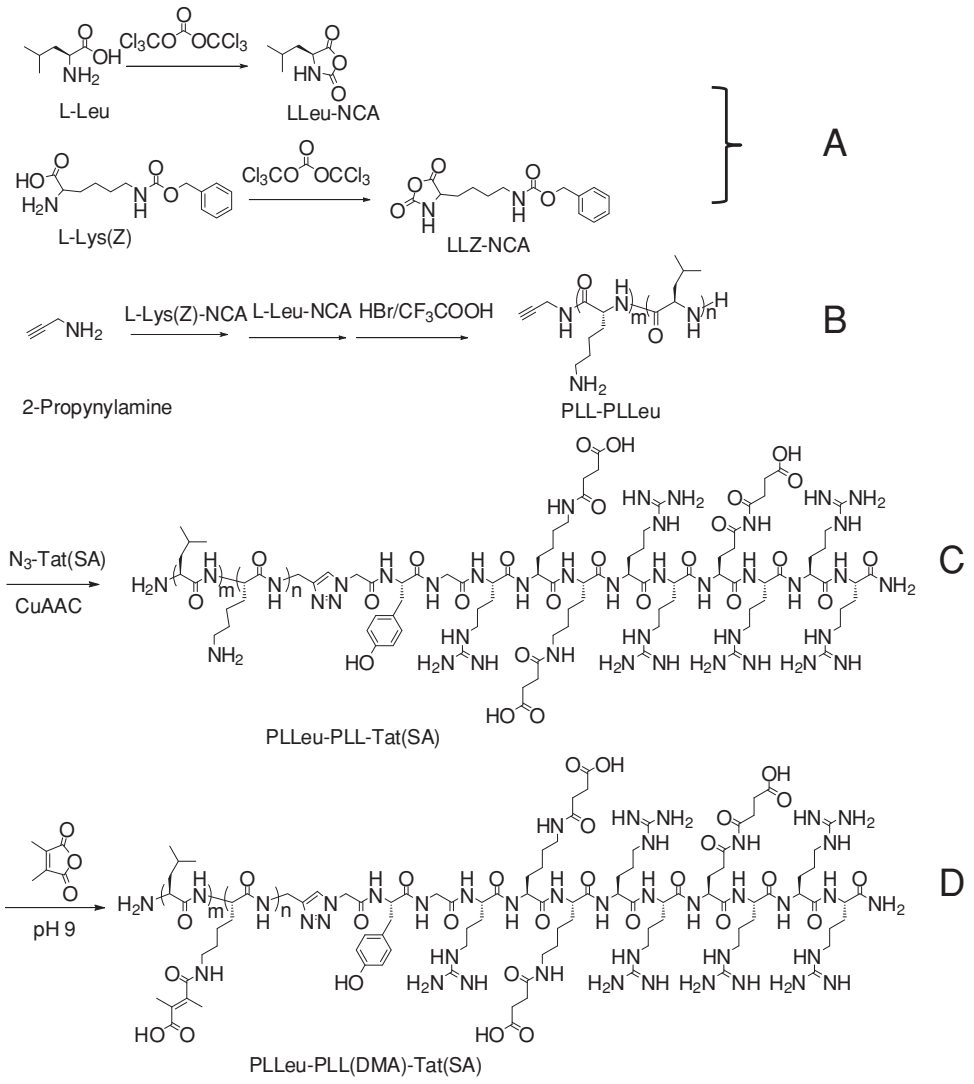

Scheme 2. Synthesis route of PPDTS. A) Synthesis of the NCA of leucine and lysine. B) Stepwise ROP of LLZ–NCA and LLeu–NCA and the subsequent deprotection. C) CuAAC click reaction conjugating the diblock polypeptide with Tat(SA). D) Amidating of the lysine amino residues of polylysine into β-carboxylic amide.

acid-labile β-carboxylic amide which was more sensitive to acid that would hydrolyze at mildly acidic conditions such as pH 6.5. The ^{1}H NMR spectrum of PPDTS was shown in **Figure 2**. The main resonance signals were well signed to the corresponding protons, indicating the successful synthesis. The facile amidating reaction between lysine amino groups and DMA was further confirmed by the ^{1}H NMR spectrum of PLLeu–PLL(DMA) (PPD) (Figure S3, Supporting Information), which demonstrated that most (approximately 82.4%) lysine amino residues were converted to the acid-labile β-carboxylic amide. The successful amidating reaction was also confirmed by their negative charge of PPDTS nanoparticles determined by zeta potential measurement (data shown and discussed below).

2.2. Characterization of PPDTS Micelle

The PPDTS is designed to be amphiphilic to self-assemble into micellar structure. The hydrophobic polyleucine blocks constitute the inner core and polylysine blocks form the hydrophilic shell, while Tat(SA) peptides act as the outer corona. To ensure it the critical micelle concentration (CMC) of PPDTS was determined by pyrene fluorescent probe method. As demonstrated in Figure S3, Supporting Information, PPDTS could assemble into micelles at both pH 9.0 and pH 5.0, which, respectively, represent the status before and after the amide hydrolyzation. The CMC values were determined to be 5.04 and 19.45 mg L^{-1}, respectively. The higher CMC value at pH 5.0 indicated that the micelles probably were less stable after the hydrolyzation of β-carboxylic amide.

A widely used antitumor drug DOX was used as the hydrophobic model drug and loaded in PPDTS micelles by a dialysis method. The drug loading content (weight percentage of drug) was determined to be 15.6%. DOX loaded PPD micelle was also fabricated as a negative control without additional Tat peptide, and its DOX loading content was 14.8%. The morphology and size of PPDTS micelles and DOX loaded PPDTS (PPDTS/DOX) was studied by transmission electronic microscopy (TEM) and dynamic

DOI: 10.1002/smll.201402865

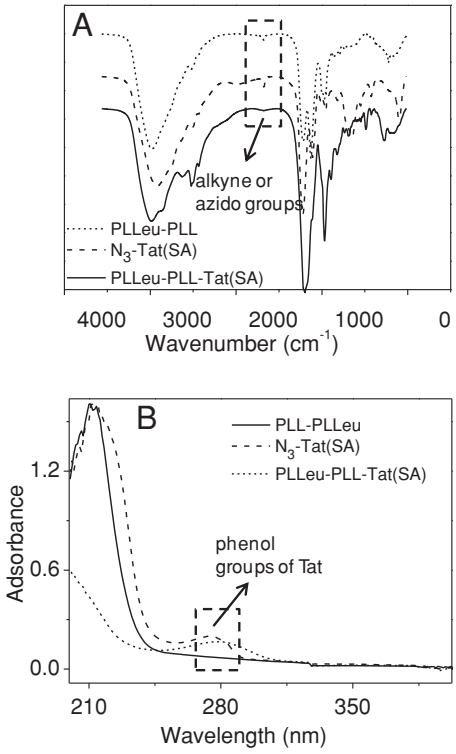

Figure 1. FTIR spetra A) and UV–vis spectra B) of PLLeu–PLL, N_3–Tat(SA), and PPTS.

light scattering (DLS), respectively. The TEM images (Figure S4A, Supporting Information) showed that both micelles had regular spherical shapes with diameter of about 20 nm, which were in consistent with the results determined by DLS (Figure S4B, Supporting Information).

2.3. Charge Reversal Behavior of PPDTS Nanoparticles

To demonstrate the charge reversal behavior of PPDTS nanoparticles at mild acidic tumor extracellular environments, the zeta potentials of PPDTS micelles at pH 7.4 and 6.5 were measured as a function of incubation time. As illustrated in **Figure 3**, the original zeta potentials of PPDTS nanoparticles were both negative in pH 7.4 and 6.5. However, when incubated at pH 6.5, the zeta potential increased quite rapidly that it became positive within just 10 min. It was because the DMA amide could be rapidly hydrolyzed at mildly acidic environment as illustrated by the NMR experiment of PPDTS in pH 6.5 (Figure S6, Supporting Information), which in result transformed the negatively charged β-carboxyl groups to positively charged amino groups. When incubated in pH 7.4, the zeta potential also increased but in a much slower speed and remained negative in more than 1 h. These phenomena were also in good consistent with literature report.[15,17] Thus the DMA modified polypeptide nanoparticles displayed a charge reversal behavior when exposed to mildly acidic environment.

2.4. Cellular Uptake and Protein Adsorption of PPDTS Nanoparticles

Due to the significant role of surface charge of nanoparticles in cell internalization and interaction with the blood proteins, this charge reversal property was expected to endow the nanoparticles with a relative selectivity in cellular uptake between normal tissues (pH 7.3–7.4) and tumor tissues (pH 6.2–6.9). Herein, culture mediums of two pHs were used to simulate the neutral normal tissue and mildly acidic tumor

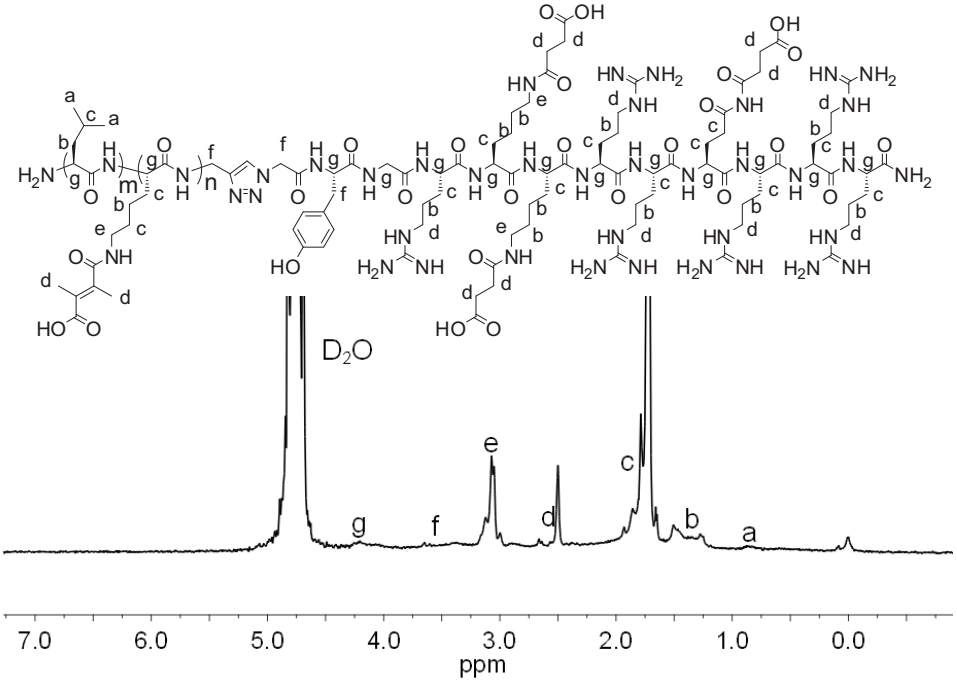

Figure 2. The ^{1}H NMR spectrum of PPDTS in D_2O.

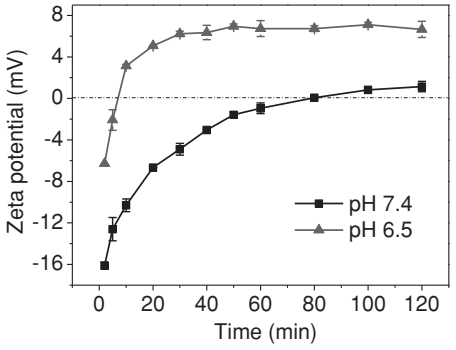

Figure 3. Zeta potential of PPDTS nanoparticles (0.5 mg mL^{-1}) at pH 6.5 or 7.4 in 20×10^{-3} M PBS as a function of incubation time.

tissue extracellular environment, respectively. Hela cells were cultured with fluorescein isothiocyanate (FITC) labeled PPDTS at pH 7.4 or 6.5 for 1 h, and their cellular uptake were studied by confocal laser scanning microscopy (CLSM) and flow cytometry. FITC labeled negatively charged PLLeu–PLL(SA)–Tat(SA) (PPSTS) and positively charged PPTS were used as controls. The cellular uptake of FITC–PPDTS in pH 7.4 and 6.5 were also investigated in Cos7 cells as a cell control.

As shown in **Figure 4**, the PPTS–FITC nanoparticles which were positively charged at both pH 7.4 and 6.5 were internalized intensively in both pHs, while PPSTS–FITC nanoparticles which could not hydrolyze their amide bonds and maintain negatively charged in pH 6.5, were rarely internalized in both pH 7.4 and 6.5. The significantly different uptake degree confirmed the important role of surface charge in cellular uptake and implied the great significance of charge reversal in selective cell internalization. As expected, the PPDTS–FITC nanoparticles were remarkably internalized by Hela cells at pH 6.5 and distributed extensively in cytoplasm, while far less nanoparticles were internalized at pH 7.4. Very similar results were gotten when FITC–PPDTS were incubated in noncancerous cell line Cos7 cells at pH 7.4 and 6.5 as shown in Figure S7, Supporting Information. Thus the nanoparticles exhibited obvious selectivity in cellular uptake between different pH environments.

This different cellular uptake capacities induced by the charge reversal property was further confirmed by flow cytometry analysis. As shown in **Figure 5**, FITC positive cells was only 12.2% at pH 7.4, but it increased to 45.9% at pH 6.5, exhibiting a remarkable enhancement in cellular uptake. The rarely cell internalization of PPDTS at pH 7.4 also confirmed that the cell penetrating function of Tat peptide was inactivated by the succinyl amidation.

Serum proteins in blood mostly possess negative charges and readily bind onto positively charged nanoparticles via electrostatic interaction which leads to their aggregation.[36] Keeping drug nanocarriers negatively charged is beneficial for their stabilization in bloodstream. Here, bovine serum albumin (BSA) was used as a model serum protein to investigate the adsorption of PPDTS and PPSTS nanoparticles at pH 7.4 and 6.5. As shown in **Figure 6**, few BSA were adsorbed to PPSTS nanoparticles at either pH 7.4 or 6.5 due to their negative charge. Less than 20% BSA were adsorbed to PPDTS nanoparticles at pH 7.4, but approximately 60% BSA were adsorbed to PPDTS nanoparticles when incubated at pH 6.5. These BSA adsorption results further demonstrated the charge reversal property of PPDTS nanoparticles at slightly acidic environments and displayed an additional benefit in bloodstream stability.

2.5. Nuclear Delivery of PPDTS Nanoparticles

Nuclear delivery of antitumor drugs is of great potential which is expected to kill tumor cell more directly and help bypass the MDR effect. The decoration of amidated Tat peptide is expected to provide the nanoparticles a nuclear delivery function, while inhibiting its nonspecific cell penetrating behavior before being internalized by tumor cells. When the nanoparticles were internalized and arrived at the acidic cell endo/lysosomes, the succinyl amides of Tat(SA) were reported to be readily hydrolyzed and subsequently recover their nuclear localization function.[28] The nuclear delivery of PPDTS nanoparticles was investigated by CLSM analysis. Hela cells were cultured with DOX loaded PPDTS nanoparticles for 6 h, and DOX loaded PPD nanoparticles without Tat peptide were used as control. As shown in **Figure 7**, for Hela cells incubated with non-Tat PPD/DOX there was little red fluorescence from DOX in cell nuclei, but it was obviously enhanced when Hela cells were incubated with PPDTS/DOX. These results demonstrated that the PPDTS nanoparticles could promote the delivery of cargoes to cell nuclei after cell internalization. To further verify the nuclear delivery behavior of PPDTS nanoparticles, FITC labeled PPDTS and PPD nanoparticles were incubated in Hela cells and the intracellular distribution were studied. As shown in Figure S8, Supporting Information, after internalization by Hela cells, most PPDTS–FITC nanoparticles were distributed in the nucleus or very close to the nuclear membrane. In contrast, the non-Tat PPD–FITC nanoparticles were completely in the cytoplasm and no FITC could be found in nucleus. These distinct results gave a direct evidence of the nuclear targeted delivery of PPDTS nanoparticles.

The nuclear delivery behavior was further studied by quantitative study of DOX accumulation in cell nuclei. As shown in **Figure 8**, after incubation for 8 or 24 h, the DOX quantity in cell nuclei for PPDTS/DOX incubation was obviously larger than that for PPD/DOX incubation, indicating the enhanced nuclear uptake by PPDTS nanoparticles. The results above demonstrated that PPDTS could definitely enhance the nuclear uptake of nanoparticles.

2.6. In Vitro Drug Release

The drug release behavior of DOX loaded PPDTS nanoparticles at pH 7.4, 6.5, and 5.0 were investigated, respectively. As shown in Figure S9, Supporting Information, the DOX release was slow at pH 7.4 that 30% of drugs were released over 12 h and 42% for 48 h, and it was similar at pH 6.5 with just a slight increase. Incubation of nanoparticles at pH 5.0 resulted in faster DOX release that 41% of drugs

DOI: 10.1002/smll.201402865

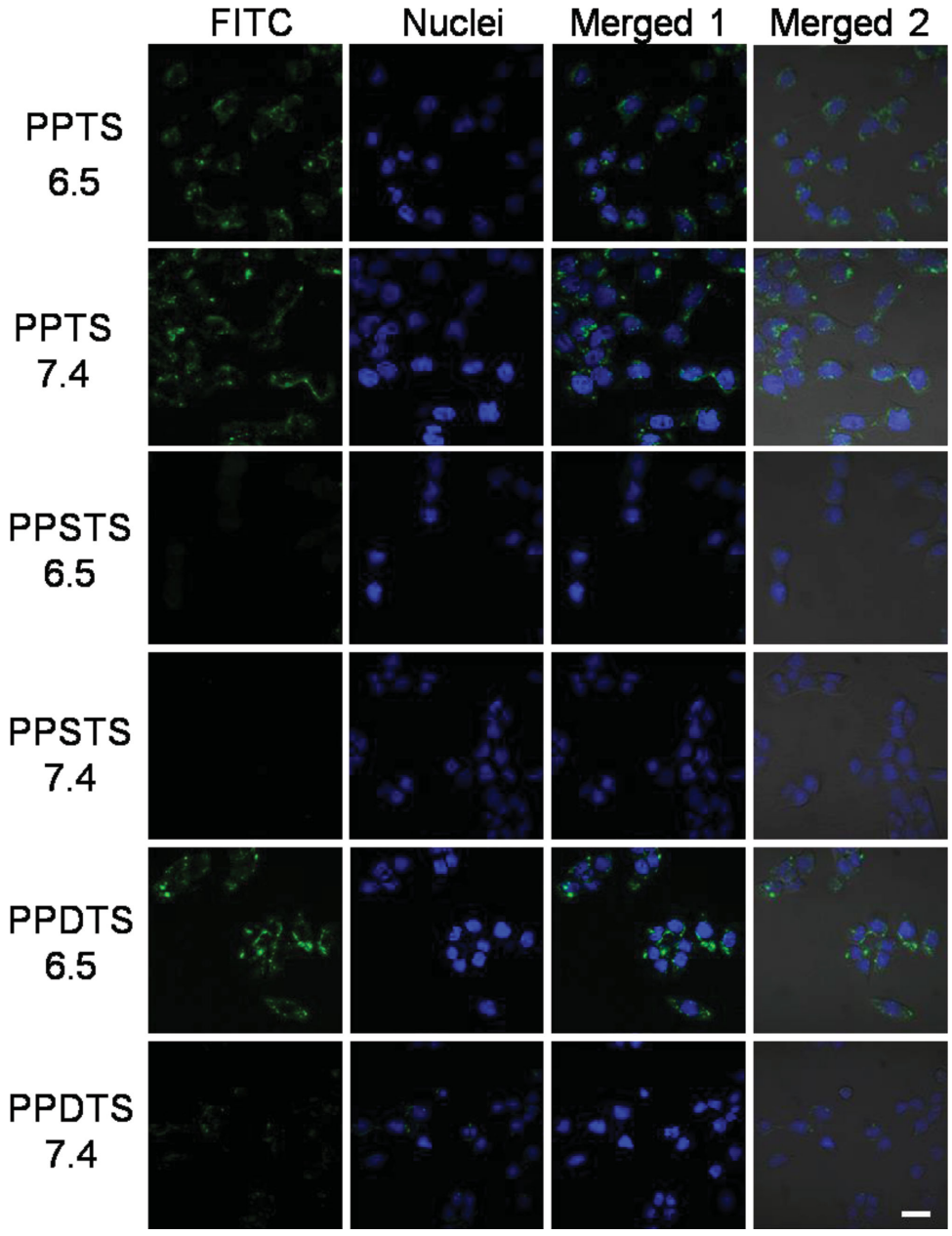

Figure 4. CLSM images of HeLa cells incubated with positively charged PPTS, negatively charged PPSTS, and charge reversal PPDTS samples at pH 6.5 or 7.4 for 1 h. PPTS, PPSTS, and PPDTS samples were labeled with green fluorescent FITC and nuclei were stained blue by Hoechst 33342. Merged 1: FITC field plus nuclei field; merged 2: FITC field and nuclei field plus bright field. Scale bar = 20 μm.

were released in 12 h and 60% for 48 h. These results were in consistent with the CMC values of PPDTS which was larger at pH 5.0 and implied a more unstable micellar structure. The faster release at pH 5.0 may also resulted from the improved solubility of DOX at acidic environment.

2.7. In Vitro Cytotoxicity

The in vitro cytotoxicity of PPDTS and DOX loaded PPDTS nanoparticles were estimated by 3-[4,5-dimethylthiazol-2-yl]-2,5-diphenyltetrazolium-bromide (MTT) assay at various nanoparticles/DOX concentrations. As shown in Figure S10A, Supporting Information, PPDTS nanoparticles showed little cytotoxicity with the cell viability higher than 85% at a concentration of 110 μg mL^{-1}, indicating the good biocompatibility, while the non-Tat control PPD nanoparticles showed a slightly higher cytotoxicity. The cytotoxicity of DOX loaded PPDTS at pH 7.4 and 6.5 to Hela cells after treating for 1 h and subsequent 48 h incubation were demonstrated in **Figure 9**A. The viability of Hela cells at pH 6.5 was obviously lower than that at pH 7.4 because of the promoted cell internalization proved above. The viability of Cos7 cells treated with PPDTS/DOX at pH 7.4 and 6.5 showed the same trend (Figure S10B, Supporting Information). These results were consistent with the selective cellular uptake at different pH induced by charge reversal behavior. The cytotoxicity of PPD/DOX as a non-Tat control was also investigated. Hela

DOI: 10.1002/smll.201402865

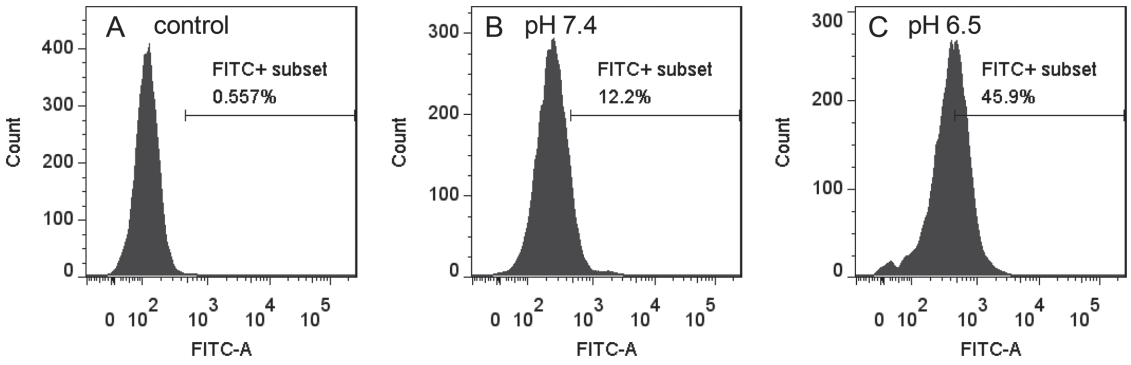

Figure 5. Flow cytometry analysis of Hela cells incubated with PPDTS–FITC at pH 7.4 B) or 6.5 C) for 1 h. Hela cells incubated without PPDTS–FITC was used as control A).

cells were treated with PPDTS/DOX or PPD/DOX at various DOX concentrations for 8 h and further incubated for 48 h before MTT analysis. As presented in Figure 9B, the cytotoxicity of PPDTS/DOX was larger than the non-Tat control because of the promoted delivery of DOX to cellular nuclei and more direct killing cells. These cytotoxicity results further demonstrated the advantages of charge reversal targeting uptake and nuclear delivery of drugs and indicated the promising application of PPDTS micelle in drug delivery for tumor therapy.

3. Conclusions

In summary, we designed a polylysine-block–polyleucine diblock polypeptide micelle decorated with Tat peptide, and the lysine amino residues of Tat and polylysine were, respectively, modified into two different β-carboxylic amides. The amides were demonstrated to stepwise hydrolyzed responding to acidic tumor extracellular environments (pH ≈ 6.5) and more acidic cell endo/lysosomes (pH ≈ 5.0), respectively, by which the amino groups and their original functions were recovered. The zeta potential measurements and in vitro cellular experiments proved that the PPDTS nanoparticles exhibited a dual-pH sensitive charge reversal behavior that they were specifically internalized by cells at tumor mildly acidic environment and directly transported into cell nuclei. Further investigations might be needed to depress the predisassembly before reaching cell nuclei so as to significantly enhance the therapeutic efficiency. Overall, this double amidation charge reversal strategy helps to realize the tumor targeting uptake and nuclear delivery simultaneously and thus provides a promising method for drug delivery in tumor chemotherapy.

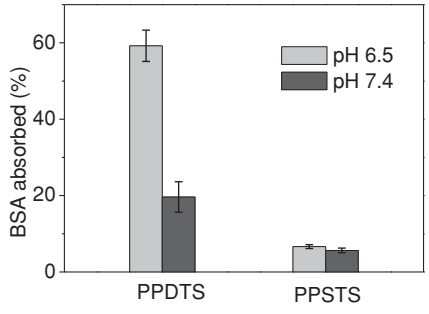

Figure 6. BSA adsorption of charge reversal PPDTS or negatively charged PPSTS at pH 6.5 or 7.4 after incubation at 37 °C for 2 h. Data are shown as mean ± SD (n = 3).

4. Experimental Section

Materials: Rink Amide-AM resin (100–200 mesh, loading: 0.59 mmol g^{-1}), *N*-diisopropylethylamine (DIEA), piperidine, 1-hydroxybenzotriazole (HOBt), *o*-benzotriazole-*N*,*N*,*N*′,*N*′-tetramethyluroniumhexafluophosphate (HBTU), L-leucine (LLeu), LLZ and *N*-Fluorenyl-9-methoxycarbonyl protected amino acids (Fmoc-Arg(Pbf)-OH, Fmoc-Gln(Trt)-OH, Fmoc-Lys(Boc)-OH, Fmoc-Gly-OH, Fmoc-Tyr(tBu)-OH) were purchased from GL Biochem. Ltd. (Shanghai, China). Succinyl chloride and DMA were purchased from Aladdin Reagent Co. Ltd. (Shanghai, China). Triphosgene was purchased from J&K Scientific (Beijing, China) and recrystallized by diethyl ether prior to use. Tris(3-hydroxypropyltriazolylmethyl) amine (THPTA) and CuBr were synthesized in prior work of our group.[37] Propargyl amine, trifluoroacetic acid (TFA), DMF and tetrahydrofuran (THF) were of analytical grade and distilled before use. DOX hydrochloride was provided by Zhejiang Hisun Pharmaceutical Co. (China). Dulbecco's Modified Eagle's Medium (DMEM), fetal bovine serum (FBS), penicillin, streptomycin, were purchased from Invitrogen (CA, USA). MTT and Hoechst 33342 were purchased from Lonza Co. (USA). All other reagents and solvents were obtained from Shanghai Reagent Chemical Co. and used directly.

Synthesis of LLZ–NCA and LLeu–NCA: LLZ–NCA and LLeu–NCA were prepared by Fuchs-Farthing method using triphosgene according to literature reports.[30,31] For LLeu–NCA synthesis, L-leucine (2.6 g, 20×10^{-3} M) was dissolved in freshly prepared dry THF (90 mL) in a three-necked flask. Then the flask was charged with steady flow of N_2 to ensure anhydrous environment and triphosgene (2.5 g, 8.4×10^{-3} M) solution in THF (10 mL) was added dropwise under vigorous stirring at 50 °C. The reaction was stopped when the mixture turned to a clear solution. Subsequently the solution was poured into excess petroleum ether to obtain crude crystals of LLeu–NCA, which was further recrystallized from THF/*n*-hexane twice, filtrated, and dried in vacuum. LLZ–NCA was synthesized with the similar procedure above.

Synthesis of Propargyl-Terminated Diblock Copolymer PLL–PLLeu: PLL–PLLeu was synthesized by stepwise ROP of LLZ–NCA and LLeu–NCA using propargyl amine as initiator. First, propargyl-

DOI: 10.1002/smll.201402865

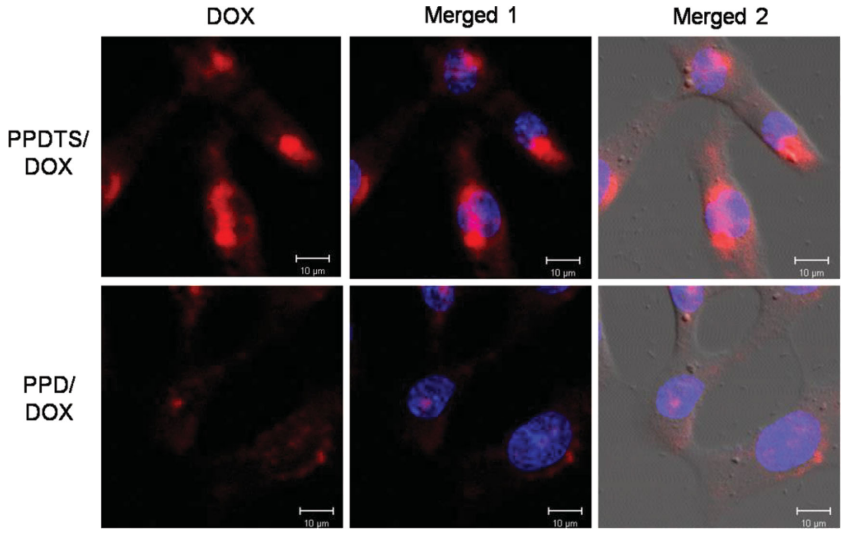

Figure 7. Confocal images of Hela cells incubated with PPD/DOX or PPDTS/DOX for 6 h . The concentration of DOX was 5.0 μg mL^{-1}. Merged 1: DOX field plus nuclei field; merged 2: DOX field and nuclei field plus bright field. Scale bar = 10 μm.

terminated PLLZ was synthesized by ROP of LLZ–NCA initiated by propargyl amine in dried DMF with certain ratio. The solution was stirred at 40 °C under N_2 atmosphere for 3 days and then precipitated by diethyl ether twice and dried under vacuum to acquire PLLZ white powders. Second the PLLZ–PLLeu copolymer was prepared by further ROP of LLeu–NCA using PLLZ as initiator. Given amount of PLLZ and LLeu–NCA were dissolved in dried DMF and stirred under N_2 atmosphere for 3 days. The product was purified by repeated precipitation in excess diethyl ether and dried under vacuum.

PLL–PLLeu was obtained by the deprotection of PLLZ–PLLeu. PLLZ–PLLeu was dissolved in TFA in an ice bath and a 33% solution of HBr in acetic acid was added dropwise. The mixture was stirred at 0 °C for 1 h and subsequently precipitated by diethyl ether, centrifuged, and dried in vacuum. The crude product was further purified by dialysis in a dialysis bag (molecular weight cut-off (MWCO) = 3500) against distilled water for 48 h, during which the water was refreshed every 6 h. PLL–PLLeu was obtained after lyophilized.

Synthesis of Azido-Terminated Tat Peptide N_3YGRKKRRQRRR (N_3–Tat): N_3–Tat was synthesized manually by the standard Fmoc SPPS protocol using Rink Amide AM resin.[33] Briefly, peptide

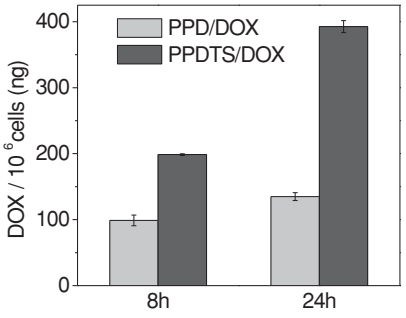

Figure 8. Quantitative study of nuclear delivery behavior of PPDTS nanocarrier: the nuclear accumulation of DOX for HeLa cells incubated with PPD/DOX or PPDTS/DOX for 8 h or 24 h. Data are shown as mean ± SD (n = 3).

chains were grown on Rink Amide AM resin in a stepwise manner at room temperature with distilled anhydrous DMF as solvent. Twenty percent piperidine in DMF (v/v) was employed to remove the Fmoc protecting group, while amino acid coupling was carried out with 4 equiv of Fmoc amino acid, HBTU, HOBt and 8 equiv of DIEA in DMF solution for 2 h, and the ninhydrin assay was used to monitor the coupling efficiency. The azide group was conjugated by reaction with 2-azidoacetic acid at the end with the same method. After that the resin was washed with DMF, methanol, and dichloromethane three times each and dried under vacuum for 4 h. The peptide was gotten by cleavage from the resin and fully deprotected simultaneously using a cleavage cocktail of TFA, thioanisole, H_2O, phenol and 1,2-ethanedithiol in a volume ratio of 83: 4.3: 4.3: 6.3: 2.1 for 2 h. The filtrate was collected, concentrated by rotary evaporation, and then precipitated into excess cold ether. The obtained precipitation was further washed with cold ether four times to remove the cleavage residuals and impurities. After that the precipitation was dissolved in distilled water and freeze dried to obtain the final peptide.

Synthesis of Succinyl Amidated N_3–Tat(SA): N_3–Tat was amidated by succinyl chloride according to a previous report.[28] N_3–Tat (0.2 g) was dissolved in 10 mL phosphate buffered solution (PBS) (pH 8.5, 50×10^{-3} M) and cooled to 0 °C. Succinyl chloride (0.5 mL) was added dropwise to the solution and about 4 equiv of NaOH was added to maintain the pH around 8.5. After reacting overnight at 0 °C, the mixture was loaded into a dialysis bag (MWCO 1000) and dialyzed against distilled water of which the pH was adjusted around 8.5 by 0.1 M NaOH solution for 24 h, and the water was changed every 4 h. The following solution was lyophilized to obtain the N_3–Tat(SA).

Synthesis of PPTS by Click Reaction: PPTS was synthesized by conjugating of PLL–PLLeu with N_3–Tat(SA) by copper (I) catalyzed azide-alkyne cycloaddition reaction. PLL–PLLeu (150 mg) and N_3–Tat(SA) (50 mg) were dissolved in distilled water (10 mL) and charged with constant N_2 under magnetic stirring. Then CuBr (30 mg) and THPTA (40 mg) were added to get a celadon solution. After reaction for 24 h, the solution was loaded into a dialysis bag (MWCO 3500) and dialyzed against ethylenediaminetetraacetic acid (EDTA) solution of which the pH was adjusted around 8.0 by NaOH. The water was changed every 4 h until the solution became colorless. The subsequent solution was freeze dried to obtain the PPTS.

Synthesis of PPDTS, PPD, and PPSTS: PPDTS was prepared by modifying the lysine amino residues of PLL blocks into β-carboxylic amide using DMA according to previous literature.[17] PPTS (40 mg) and three equivalents (to amino groups) of DMA (80 mg) were dissolved in distilled water and NaOH was added to the solution to maintain the pH around 10.0. After reaction for 12 h, the solution was purified by dialysis (MWCO 3500) against slightly basic water (pH 9–10) and freeze dried. The FITC labeled samples were prepared directly reacting between its amino group and FITC in dark for 6 h and subsequently dialysis and lyophilized. PPD was

DOI: 10.1002/smll.201402865

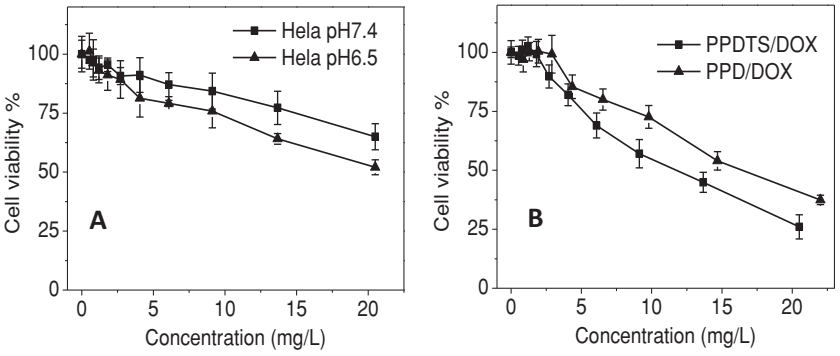

Figure 9. Cell viability of Hela cells treated with A) PPDTS/DOX at pH 7.4 or 6.5 for 1 h and further incubated of 48 h; B) PPDTS/DOX or PPD/DOX for 8 h and further incubated for 48 h. Cell viability were determined by MTT assay at various DOX concentrations (mean ± SD, $n = 4$).

synthesized by PLL–PLLeu and DMA in the similar method. PPSTS was synthesized by PPTS and succinyl choloride similar to that of N_3–Tat(SA).

Preparation of DOX Loaded PPDTS and PPD: A widely used antitumor drug DOX was chosen as the model drug. DOX hydrochloride (10 mg) was dissolved in 3 mL of DMSO and triethylamine (0.15 mL) was added to remove the HCl of the DOX hydrochloride. PPDTS (50 mg) was added to the solution and stirred in dark for 4 h. Then the solution was added dropwise to 5 mL PBS (pH 9.5) and stirred for another 3 h. After that the solution was loaded into a MWCO 3500 dialysis bag and dialyzed against pH 9–10 water until there was almost no DOX in the dialyzed water monitored by fluorescence spectroscopy. The obtained solution was mildly centrifuged and the supernatant was stored in 0 °C which would be used directly. The DOX loading content was determined by lyophilizing 1.0 mL of the above solution and dissolved the obtained powder in DMSO. The DOX concentration was measured by fluorescence analysis (emission wavelength at 560 nm, excitation wavelength at 488 nm). The DOX loaded PPD was fabricated with the similar procedure.

Characterizations: The molecular mass of peptide N_3–Tat and N_3–Tat(SA) was determined by the MALDI–TOF on an Axima TOF^2 mass spectrometer (Shimadzu, Kyoto, Japan). Every step synthesizing PLL–PLLeu and the final product PPDTS were monitored by ^{1}H NMR recorded on a Varian Mercury VX 300 MHz spectrometer using DMSO-d_6 or D_2O as the solvent and tetramethylsilane (TMS) as the internal standard. Molecular weight of polypeptide was determined by GPC system equipped with a Waters 2690D separations module and a Waters 2410 refractive index detector. DMF was used as the eluent solution and polystyrene as standard. The success of the click reaction was characterized by FTIR collected on a Perkin-Elmer spectrophotometer (USA) using potassium bromide pellet, and UV–vis was also performed on a Lambda Bio 40 UV–vis spectrometer (Perkin-Elmer, USA).

The zeta potential, hydrodynamic particle size, and size distribution were measured by DLS on a Malvern Zetasizer Nano-ZS ZEM3600 apparatus (UK). Morphology observation of micelles was performed by TEM with a JEM-100CX II microscopy at an acceleration voltage of 100 kV and the samples were negatively stained by phosphotungstic acid. Fluorescent measurement was performed on a RF-530/PC fluorescence spectrometer.

Determination of CMC: The CMC value of PPDTS was determined by fluorescence spectroscopy using pyrene as a hydrophobic probe. Pyrene solution in acetone (100 µL, 6×10^{-6} M) was added into a series of centrifugal tubes, and the acetone was allowed to evaporate. Then 1.0 mL of PPDTS aqueous solution of various concentrations was added to the above tubes, shaked vigorously, and kept overnight. The final concentration of pyrene was 6×10^{-7} M, exceeding the saturation solubility of pyrene in water at room temperature. Emission wavelength was carried out at 390 nm and excitation spectra were recorded ranging from 300 to 360 nm. Both emission and excitation slit widths were 5 nm. A redshift of excitation peak arose around 335 nm. The intensity ratios as a function of logarithm of the PPDTS concentrations were analyzed and plotted. The CMC value was determined from the intersection of the tangent to the curve at the inflection with the horizontal tangent through the points at low concentration.[3]

Changes of Zeta Potential of the PPDTS Micelles at Different pHs: The PPDTS was dispersed in pH 7.4 and 6.5 PBS (20×10^{-3} M) at the concentration of 0.5 mg mL^{-1} and incubated at 37 °C. Samples were taken at designated time intervals and the zeta potentials were measured. Each measurement was performed for three times and each time for 30 runs and the results presented are the average data.

Hydrolysis of PPDTS in pH 6.5 Monitored by NMR: The PPDTS was dispersed in PBS of pH 6.5 (20×10^{-3} M) and incubated. After certain time (0, 10, 30, and 60 min), some PPDTS solution was quickly taken out and freeze dried. The lyophilized samples were characterized by ^{1}H NMR in D_2O recorded on a Varian Mercury VX 300 MHz spectrometer. The signals around 2.9 and 3.1 ppm in the spectra were compared and analyzed.

Cellular Uptake at Different pHs Observed by CLSM: Hela cells were seeded in a glass bottom dish at a density of 1×10^5 cells per dish in 1 mL of DMEM with 10% FBS and 1% antibiotics (penicillin–streptomycin, 10 000 U mL^{-1}). The cells were incubated at 37 °C in a humidified atmosphere containing 5% CO_2 for 24 h. Then the culture medium was replaced by fresh DMEM containing FITC–PPDTS, FITC–PPSTS, or FITC–PPTS at the equivalent sample concentration of 30 µg mL^{-1} at pH 7.4 or 6.5, respectively. After incubation for 1 h at 37 °C, the cells were washed five times with PBS. Subsequently the cell nuclei were stained by Hoechst 33342 for 15 min and washed three times with PBS. The cellular uptake of samples was visualized under a laser scanning confocal microscope (C1-Si, Nikon, Japan). The measurements of cellular uptake of FITC–PPDTS in Cos7 cells at pH 7.4 or 6.5 were also investigated with the same method.

Cellular Uptake at Different pHs Measured by Flow Cytometry: Hela cells were seeded onto a six-well plate at a density of 5×10^4 cells per well and cultured for 24 h. Then the culture medium was removed and replaced with DMEM (pH 7.4 or 6.5) containing FITC–PPDTS at concentration of 40 µg mL^{-1} and the cells were further incubated for 1 h at 37 °C. The medium was removed and the cells were washed thrice with PBS. Then 0.5 mL of trypsin was added to each well to digest the cells. The cells were collected and centrifuged at 1000 rpm for 3 min. The supernatant was removed and the cells at the bottom were washed once, centrifuged again, and resuspended in PBS. After been filtrated the cells were quickly

DOI: 10.1002/smll.201402865

examined by flow cytometry (BD FACS Aria III, USA). Cells cultured at pH 7.4 DMEM without FITC–PPDTS was used as negative control.

Protein Adsorption of the Micelles: BSA was used as model protein to determine the protein adsorption ability of the PPDTS and PPSTS at different pHs.[18] The PPDTS/PPSTS were incubated with 1 mL of BSA solution in PBS at pH 7.4 or 6.5 with the final concentration of micelles and protein at 0.2 and 0.4 mg mL^{-1}, respectively. After incubation at 37 °C for 1 h, each sample was centrifuged at 8000 rpm for 15 min to precipitate the protein adsorbed aggregates, and the supernatant was carefully collected. The protein concentration of supernatant was determined by UV–vis spectroscopy by measuring its characteristic UV absorbance at 280 nm, and compared to the standard curve obtained from BSA solutions of known concentrations. Then, the adsorbed proteins on the samples were calculated as the degree adsorbed.

Nuclear Localization of DOX Measured by CLSM: Hela cells were seeded in a glass bottom dish at a density of 1×10^5 cells per dish and incubated at 37 °C for 24 h. Then the culture medium was replaced by fresh DMEM containing PPDTS/DOX or PPD/DOX at the equivalent DOX concentration of 5 μg mL^{-1} at pH 6.5, respectively. After incubation for 6 h at 37 °C, the cells were washed three times with PBS. Subsequently the cell nuclei were stained by Hoechst 33342 and washed with PBS. The nuclear uptakes of DOX were visualized under a confocal microscope.

Nuclear Delivery of FITC Labeled Nanoparticles Measured by CLSM: Hela cells were cultured as above and treated with PPDTS–FITC and PPD–FITC for 6 h at 37 °C. Then the cells were washed three times with PBS. Subsequently the cell nuclei were stained by Hoechst 33342 and washed with PBS. The intracellular distribution of FITC labeled nanoparticles were observed under a confocal microscope.

Quantitative Studies of DOX Accumulation in Cell Nuclei: Hela cells were seeded onto six-well plates at a density of 1×10^5 cells per well and cultured in DMEM with 10% FBS at 37 °C. After incubation for 24 h, the cells were cultured in DMEM containing PPDTS/DOX or PPD/DOX at DOX concentration of 10 μg mL^{-1} for 8 or 24 h. Then the cells were washed with PBS three times and trypsin digested. After centrifugation at 1400 rpm for 3 min, the cells were resuspended in PBS and washed twice. Then the concentrations of cells were counted with a hemocytometer. Subsequently, nuclei were isolated from cytoplasm by disrupting cell membranes using surfactants and further centrifugation as follows. The cells were suspended in lysis buffer of 100×10^{-3} M NaCl solution with 1×10^{-3} M EDTA, 1% Triton X-100 and 10×10^{-3} M Tris buffer (pH 7.4) at 4 °C for 10 min. The suspension was then centrifuged at 4000 rpm for 6 min to separate the cell nuclei from the plasma membrane fragments. Then the precipitate of cell nuclei was collected and suspended in lysis buffer again and disrupted by ultrasound for 0.5 h. The amount of DOX in the cell nuclei was determined by fluorescence measurement.

In Vitro *Release of DOX from PPDTS/DOX*: The release behavior of DOX from PPDTS/DOX was investigated in three different mediums, namely, pH 7.4 phosphate buffer (20×10^{-3} M), pH 6.5 phosphate buffer (20×10^{-3} M), and pH 5.0 acetate buffer (20×10^{-3} M). PPDTS/DOX aqueous solution (0.5 mL) was added to each dialysis bag (MWCO 3500). The dialysis bags were immersed in 10 mL of the above three buffers, respectively, and kept in 37 °C bath with constant shaking (200 rpm). At predetermined time the whole medium was collected and resupplied with 10 mL fresh medium. The buffer collected was subjected to fluorescence analysis to determine the DOX concentration. The fluorescence spectroscopy was measured at emission wavelength of 560 nm and excited at 488 nm, using a standard calibration curve experimentally obtained. The experiments were carried out in triplicate and data were shown as mean ± standard deviation (SD).

Cytotoxicity Assay: The cytotoxicity of PPDTS, PPDTS/DOX, PPD, and PPD/DOX were evaluated by the MTT assay. Hela and Cos7 cells were seeded in 96-well plates at a density of 6000 cells per well in 100 μL DMEM containing 10% FBS and cultured for 24 h at 37 °C. Then the cells were treated with 100 μL culture medium of pH 7.4 or 6.5 containing fixed amount of nanoparticles for 1 or 8 h and further incubated for 48 h. After that the medium was replaced with 200 μL of fresh DMEM and 20 μL MTT (5 mg mL^{-1} in PBS) and incubated for another 4 h, allowing live cells to change the yellow tetrazolium salt into dark blue formazan crystals. Then the medium was removed and 200 μL DMSO was added. The absorbance at 570 nm was collected using a micro plantreader (Bio-Rad, Model 550, USA). The cytotoxicity was expressed as percentage of cell viability versus the control: cell viability = $OD_{sample}/OD_{control} \times 100\%$, where OD_{sample} was obtained in the presence of PPDTS or PPDTS/DOX and $OD_{control}$ was obtained in the absence of samples (OD means optical density). Data were shown as mean ± SD based on four independent experiments.

Supporting Information

Supporting Information is available from the Wiley Online Library or from the author.

Acknowledgements

We acknowledge the financial support from the National Natural Science Foundation of China (51125014 and 51233003), the Ministry of Science and Technology of China (2011CB606202), and Natural Science Foundation of Hubei Province of China (2013CFA003).

[1] R. Langer, *Nature (London)* **1998**, *392*, 5.
[2] Z. S. Ge, S. Y. Liu, *Chem. Soc. Rev.* **2013**, *42*, 7289.
[3] I. K. Kwon, S. C. Lee, B. Han, K. Park, *J. Controlled Release* **2012**, *164*, 108.
[4] K. Kim, J. H. Kim, H. Park, Y. S. Kim, K. Park, H. Nam, S. Lee, J. H. Park, R.-W. Park, I. S. Kim, K. Choi, S. Y. Kim, K. Park, I. C. Kwon, *J. Controlled Release* **2010**, *146*, 219.
[5] Y. Li, G. H. Gao, D. S. Lee, *Adv. Healthcare Mater.* **2013**, *2*, 388.
[6] N. Parker, M. J. Turk, E. Westrick, J. D. Lewis, P. S. Low, C. P. Leamon, *Anal. Biochem.* **2005**, *338*, 284.
[7] J. Y. Rao, A. Khan, *J. Am. Chem. Soc.* **2013**, *135*, 14056.
[8] J. Y. Rao, C. Hottinger, A. Khan, *J. Am. Chem. Soc.* **2014**, *136*, 5872.
[9] R. A. Cardone, V. Casavola, S. J. Reshkin, *Nat. Rev. Cancer* **2005**, *5*, 786.
[10] G. F. Luo, W. H. Chen, Y. Liu, J. Zhang, S. X. Cheng, R. X. Zhuo, X. Z. Zhang, *J. Mater. Chem. B* **2013**, *1*, 5723.

DOI: 10.1002/smll.201402865

[11] S. E. A. Gratton, P. A. Ropp, P. D. Pohlhaus, J. C. Luft, V. J. Madden, M. E. Napier, J. M. DeSimone, *Proc. Natl. Acad. Sci. USA* **2008**, *105*, 11613.
[12] Y. Lee, T. Ishii, H. Cabral, H. J. Kim, J. H. Seo, N. Nishiyama, H. Oshima, K. Osada, K. Kataoka, *Angew. Chem. Int. Ed.* **2009**, *48*, 5309.
[13] Y. Lee, T. Ishii, H. J. Kim, N. Nishiyama, Y. Hayakawa, K. Itaka, K. Kataoka, *Angew. Chem. Int. Ed.* **2010**, *122*, 2606.
[14] P. S. Xu, E. A. V. Kirk, Y. H. Zhan, W. J. Murdoch, M. Radosz, Y. Q. Shen, *Angew. Chem. Int. Ed.* **2007**, *46*, 4999.
[15] Z. X. Zhou, Y. Q. Shen, J. B. Tang, M. H. Fan, E. A. V. Kirk, W. J. Murdoch, M. Radosz, *Adv. Funct. Mater.* **2009**, *19*, 3580.
[16] J. Z. Du, T. M. Sun, W. J. Song, J. Wu, J. Wang, *Angew. Chem. Int. Ed.* **2010**, *122*, 3703.
[17] J. Z. Du, X. J. Du, C. Q. Mao, J. Wang, *J. Am. Chem. Soc.* **2011**, *133*, 17560.
[18] Y. Y. Yuan, C. Q. Mao, X. J. Du, J. Z. Du, F. Wang, J. Wang, *Adv. Mater.* **2012**, *24*, 5476.
[19] D. L. Crowe, *Recent Res. Dev. Cancer* **2002**, *4*, 65.
[20] M. A. Fuertes, J. Castilla, C. Alonso, J. M. Perez, *Recent Res. Dev. Mol. Pharmacol.* **2002**, *1*, 37.
[21] G. Szakacs, J. K. Paterson, J. A. Ludwig, C. B. Genthe, M. M. Gottesman, *Nat. Rev. Drug Discovery* **2006**, *5*, 219.
[22] H. Lage, *Cell Mol. Life Sci.* **2008**, *65*, 3145.
[23] L. M. Pan, J. N. Liu, Q. J. He, L. J. Wang, J. L. Shi, *Biomaterials* **2013**, *34*, 2719.
[24] E. Vives, P. Brodin, B. Lebleu, *J. Biol. Chem.* **1997**, *272*, 16010.
[25] S. S. Patel, B. J. Belmont, J. M. Sante, M. F. Rexach, *Cell* **2007**, *129*, 83.
[26] L. M. Pan, Q. J. He, J. N. Liu, Y. Chen, M. Ma, L. L. Zhang, J. L. Shi, *J. Am. Chem. Soc.* **2012**, *134*, 5722.
[27] J. Hoyer, I. Neundorf, *Acc. Chem. Res.* **2012**, *45*, 1048.
[28] E. L. Jin, B. Zhang, X. R. Sun, Z. X. Zhou, X. P. Ma, Q. H. Sun, J. B. Tang, Y. Q. Shen, E. V. Kirk, W. J. Murdoch, M. Radosz, *J. Am. Chem. Soc.* **2013**, *135*, 933.
[29] Z. Y. Li, H. Y. Wang, C. Li, X. L. Zhang, X. J. Wu, S. Y. Qin, X. Z. Zhang, R. X. Zhuo, *J. Polym. Sci. Pol. Chem.* **2011**, *49*, 286.
[30] A. C. Farthing, R. J. W. Reynolds, *Nature* **2014**. *65*, 647.
[31] M. Kar, P. S. Vijayakumar, B. L. V. Prasad, S. S. Gupta, *Langmuir* **2010**, *26*, 5772.
[32] A. J. Qin, J. W. Y. Lam, B. Z. Tang, *Chem. Soc. Rev.* **2010**, *39*, 2522.
[33] W. C. Chan, P. D. White, *Fmoc Solid Phase Peptide Synthesis: A Practical Approach*, Oxford, Oxford, UK **2000**.
[34] X. H. Luo, F. W. Huang, S. Y. Qin, H. F. Wang, J. Feng, X. Z. Zhang, R. X. Zhuo, *Biomaterials*, **2011**, *32*, 9925.
[35] P. E. Schneggenburger, B. Worbs, U. Diederichsen, *J. Pept. Sci.* **2010**, *16*, 10.
[36] L. Rong, L. H. Liu, S. Chen, H. Cheng, C. S. Chen, Z. Y. Li, S. Y. Qin, X. Z. Zhang, *Chem. Commun.* **2014**, *50*, 667.
[37] C. Deng, J. T. Wu, R. Cheng, F. H. Meng, H. A. Klok, Z. Y. Zhong, *Prog. Polym. Sci.* **2014**, *39*, 330.

Received: September 25, 2014
Revised: December 26, 2014
Published online:

DOI: 10.1002/smll.201402865